

## Master Sintering Curve for TiO<sub>2</sub>

**Saad B. H. Farid**

Dept. of Materials Engineering / University of Technology

**Sawsan A. H. Mahdi**

**Hanan K. H. Al.Mayaly**

Dept. of Physics / College of Education For Pure Science (Ibn Al-Haitham)/  
University of Baghdad

**Received in : 9 December 2012 , Accepted in : 17 March 2013**

### Abstract

The master sintering concept is introduced as a unifying sintering model for the initial, intermediate and final stage of sintering. The master sintering curve is independent on the time-temperature trajectory due to account for its integral. The master sintering curve is constructed on a material parameter, which is the activation energy for sintering and other curve shaping parameters, which depends on the initial state of the powder. Literature data of sintering of TiO<sub>2</sub> compacts with two initial packing densities of 55% and 69% of theoretical is utilized for the construction of the master sintering curves. The higher initial packing density compact shows higher densification rate, which is reflected by different set of shaping parameters compared with those of lower initial packing density. The master grain growth curve of TiO<sub>2</sub> compacts is also constructed which shows slower grain growth for the higher initial packing density compact.

**Key Words :** Sintering, Master Sintering Curve, TiO<sub>2</sub>

## Introduction

Sintering, as a thermal process that bonds particles together into a solid, coherent structure, by means of mass transport mechanisms, is divided into initial, intermediate and final stages [1]. In the initial stage of sintering, the interparticle contact area of the powder compact increases and the grain boundaries are formed on the expense of surface area. The intermediate stage begins at the start of the grain growth and shrinkage of the volume of the pore network. The densification continues with pore shrinkage and reaches a stage where pore phase transforms into individual closed pores assigning the final stage of sintering [1-2]. Sintering behavior of any particular material depends upon several characteristics of the powder; including composition, the particle size, and size distribution, initial powder packing, heating rate, sintering temperature, sintering time and atmosphere [3-5].

Synthesis of nanocrystalline materials powders has paid much attention due to their promising properties. The sintering of nanocrystalline materials is an important step in the fabrication process that significantly affects their final microstructure and properties [6-8].

One of the important cases of nanomaterials is  $\text{TiO}_2$  powder; it is one of the most widely used metal oxides in the nanometric sizes.  $\text{TiO}_2$  nanopowder has broad range of applications, including pigments, gas and humidity sensors, catalyst support, solar cells, and capacitors.

Thus,  $\text{TiO}_2$  has been widely studied with respect to synthesis of nano-sized powder, thin film

fabrication and sintering of nano structured  $\text{TiO}_2$  ceramics. On the other hand, the properties of sintered  $\text{TiO}_2$  ceramics are affected by their micro structural features, which originate from the initial properties like the grain size distribution and packing [9-10].

Generally, initial powder packing is an essential influencing parameter which is rarely investigated [5]; Accordingly, the aim of this study is to study the sintering behavior of nano- $\text{TiO}_2$  powder via application of the recent Master Sintering Curve theory on published data and build MSC model for sintering of  $\text{TiO}_2$  powders.

## Theoretical part

In general, the modeling of the sintering is very complicated and the developed sintering models are limited to both initial and intermediate stage or to the final stage of sintering. The first unifying sintering model that brings together the three stages of sintering is that by Hansen et al [11]. This work is followed by that of Hunghai and Johnson [12], which attempted to model the sintering process by a single equation, called the Master Sintering Curve (MSC). MSC describes densification through all stages of sintering through density as a function of time and a second parameter represents the thermal history throughout the sintering process. The model is further described and the application of methodology is explained by Teng et al [13] and Park et al [14].

Based on MSC formulations [11-14], the density  $\rho$  is described by sigmoidal (S-shaped) function as follows:

$$\rho = \rho_o + \frac{a}{[1 + \exp\left(-\frac{\log(\Theta) - \log(\Theta_o)}{b}\right)]^c} \dots \dots \dots (1)$$

$\rho_o$  is the initial density which corresponds to the lower asymptote of the curve; where the upper asymptote is  $\rho_o + a$ . The parameter b controls the densification rate and c influence near which asymptote maximum densification occurs. The parameter  $\Theta$  represents the time-temperature profile of the sintering process which is called the work of sintering, and  $\Theta_o$  is the value of  $\Theta$  at the point of inflection of the S-curve. The parameters  $\rho_o$ , a, b, c and  $\log(\Theta_o)$  are called the shape parameters of the S shaped function. The parameter  $\Theta$  is expressed in terms

as of sintering time  $t$  and the absolute sintering temperature as function of time  $T(t)$  as follows:

$$\Theta(t, T) = \int_0^t \frac{1}{T} \exp\left(-\frac{Q}{RT}\right) dt \dots \dots \dots (2)$$

The symbol  $R$  appears in equation (2) denotes the gas constant and  $Q$  is the activation energy of the sintering process. Sintering data should be utilized to fit MSC mentioned in equation 2 in order to find the activation energy of the sintering process. Once the activation energy  $Q$  is found, the density profile can be calculated for any time temperature profile utilizing the equations (1-2).

The grain growth equation that resembles the master sintering curve is as follows [15]:

$$G = \sqrt[3]{G_o^3 + 3\Theta_G} \dots \dots \dots (3)$$

$G$  represents the grain size as function of time and the initial grain size is  $G_o$ . The variable  $\Theta_G$  is expressed as follows:

$$\Theta_G(t, T) = \int_0^t K_G \exp\left(-\frac{Q_G}{RT}\right) dt \dots \dots \dots (4)$$

The shape parameter  $K_G$  and the activation energy for the grain growth  $Q_G$  can be determined by curve fitting the experimental data.

Concluding, finding the activation energy for densification  $Q$  and activation energy for the grain growth  $Q_G$  comprises the groundwork for modeling of the sintering process.

## Modeling

Experimental sintering data of  $TiO_2$  compacts obtained by Barringer and Bowen [16] were used as for modeling of sintering. The data is composed of densification and grain growth for two initial packing densities, 55% and 69% of theoretical at different sintering temperatures. Also, Microsoft Excel "Data analysis" and "Solver" built in routines are used for solving equations; in addition, the program is used to perform numerical integration and all other mathematical calculations. The reason to prefer Microsoft Excel environment is the flexibility of the program to manage data and drawing results next to it.

The density-sintering time trajectories are used to calculate  $\Theta$  by numerical integration of equation (2) with assumed activation energy  $Q$  for densification. As well, the values of  $\Theta$  is used to obtain the master sintering curves by Excel's "Solver" routine for equation (1); then the calculated densities are compared with the original (experimental) data. The above steps are repeated with different values of activation energies until reach the minimum difference between the calculated and experimental data of the densities.

Similarly,  $\Theta_G$  values are calculated via equation (3) and the experimental grain growth data. Equation (4) can be simply integrated due to that the time  $t$  is only variable on the right hand side due to that the temperature  $T$  is constant through the sintering experiment according to the experimental data. Accordingly, an expression for  $\Theta_G$  is found for each sintering experiment that is associated with sintering temperature. These expressions then solved simultaneously for  $Q_G$  and  $K_G$  utilizing Excel's "Data analysis" routines.

The primary results are finding the activation energies for densification and grain growth  $Q$  and  $Q_G$  respectively. These activation energies are principal materials parameters. The other

parameters that define the profile of densification and grain growth graphs depend on other parameters like the initial grain size. The initial packing density of the powder affects the profile of the densification and grain growth as will be shown in the results.

## Results and Discussion

The calculated master sintering curve of  $\text{TiO}_2$  powder of initial packing density of 55% of theoretical is shown in figure (1). It represents the percentage of the relative densities plotted against the natural log of the work of sintering ( $\Theta$ ). It also resembles an S shape function as expected. Three sets of sintering data of isothermal sintering at  $1060^\circ\text{C}$ ,  $1100^\circ\text{C}$  and  $1160^\circ\text{C}$  are used to construct the master sintering curve. The value of the activation energy that makes minimum difference between the experimental and calculated densities is  $226.9 \text{ kJ mol}^{-1}$ . The activation energy and the shape parameters for the  $\text{TiO}_2$  compacts are listed in table (1).

The master sintering curve of  $\text{TiO}_2$  powder of initial packing density of 69% of theoretical is presented in figure (2). In addition, shape parameters are shown in table (2). The model values of the parameter  $\rho_0$  shown in the table is not exactly 55% and 69% but slightly different which reflects the best calculated or model values that are expected for compacts.

In both figures (1) and (2), the equation of the master sintering curve is listed at the top of the figure. Comparing the two figures shows that the higher initial packing density squeezes the S shape by pushing its base upward and pushing the start of the growth to the right.

Note that the work of sintering ( $\Theta$ ) contains the effect of temperature  $T$  as shown in equation (2); thus, all temperatures are included in the same master sintering curve, i.e. the master sintering curve is independent of the sintering temperature. In order to see the densification behavior for each sintering time separately, figure (3) is plotted as percentage of the relative density versus time. The figure shows both experimental densities and that is calculated with the aid of the master sintering curve.

The densification rate is increased as the sintering temperature increased as shown in figure (3). The figure also shows that the higher packing density significantly increases the densification rate.

The calculations of the master sintering curves for grain growth yields activation energy for grain growth of  $288013.3 \text{ kJ mol}^{-1}$  and different shape parameter  $K_G$  for each initial packing density of  $\text{TiO}_2$ . These data is listed in table 2. Additionally, a plot of the relative grain size  $G/G_0$  versus the percentage of the relative density is shown in figure (4). The figure shows that same grain size-density trajectory is for different sintering time but the higher packing leads to slower grain growth for the sintered  $\text{TiO}_2$  compacts.

## Conclusion

1. The master sintering curves are built for  $\text{TiO}_2$  compacts for different packing densities. The master sintering curves represents the entire sintering process including initial, intermediate and final stage of sintering.
2. The densification rate is increased as the sintering temperature increased and the higher packing density significantly increases the densification rate for the  $\text{TiO}_2$  compacts.
3. The grain growth for the sintered  $\text{TiO}_2$  compacts is independent on the sintering temperature but slower grain growth is observed with higher initial packing density.

## References

1. Zhao, J. and Harmer, M.P.(1988 ), Effect of pore distribution on microstructure development: I, Matrix pores, J. Am. Ceram. Soc. 71, 2,113-20 .
2. Wong, B. and Pask, J. A.( 1979), Models for Kinetics of Solid State Sintering, J. Amer. Ceram. Soc. 62,138

3. Zhao, J. and Harmer, M.P.(19880, Effect of pore distribution on microstructure development: II, First and second generation pores, J. Am. Ceram. Soc. 71, 7, 530-39
4. Wang, Q.B.; Wang, Q.G. and Wan2\*, C.X, 2010 , Effect of Sintering Time on the Microstructure and Properties of Inorganic Polyphosphate Bioceramics. Science of Sintering, 42,337-343.
5. Bjørk, R.; Tikare, V.; Frandsen, H. L.; and Pryds, N. (2012) , The sintering behavior of close-packed spheres, Scripta Materialia 67, (81–4)
6. Ebrahimi, F.( 2012) , Nanocomposites - New Trends and Developments, InTech Publishing, New York, USA .
7. Neralla, S.(2012), Nanocrystals - Synthesis Characterization and Applications, InTech Publishing, New York, USA .
8. Hashim, A. A.( 2012) , Smart Nanoparticles Technology, InTech Publishing , New York, USA .
9. Sheng, C.; Vladimir, P. and Fatih, D, ( 2010) , Effects of sintering temperature on the microstructure and dielectric properties of titanium dioxide ceramics, J.Mat. Sci.45, 24, 6685-93.
10. Mahdi, E. M.; Hamdi, M. and Yusoff, M. S. M.( 2012) , The Effect of Sintering on the Physical and Optical Properties of Nano-TiO2 Synthesized Via a Modified Hydrothermal Route, Arab J. Sci. Eng.,1-11.
11. Hansen, J. D.; Rusin, R. P.;Teng, M-H and Johnson, D. L.(1992), Combined-Stage Sintering Model, J. Am. Ceram. Soc., 75, 5, 1129-35 .
12. Hungchai, S. and Johnson, D. L.(1996) , Master Sintering Curve: A Practical Approach to Sintering, J. Am. Ceram, Soc., 79, 12, 3211-17.
13. Teng, M. H.;Lai ,Y. C.and Chen ,Y. T.(2002) , A computer Program of Master Sintering Curve Model to Accurately Predict Sintering Curves, Western Pacific Earth Sciences, 2, 2, 171-80.
14. Park, S. J.; Chung, S. H.; Blaine, D.;Suri, P.and German, R. M.(2004), Master Sintering Curve: Construction Software and its Applications, Advances in: Powder Metallurgy and Particulate Materials, MPIF, Princeton, NJ.
15. Bollina, R. (2005), In Situ Evaluation of Supersolidus Liquid Phase Sintering Phenomena of Stainless Steel 316l: Densification and Distortion, Ph.D. Thesis, The Pennsylvania State University, The Graduate School, PSU
16. Barringer, E. A. and Bowen, H. K. (1988), Effects of Particle Packing on the Sintered Microstructure, Appl. Phys. A 45, 271-5.

**Table No. (1) : The Master sintering and grain growth curve parameters for TiO<sub>2</sub> compacts**

The master sintering curve			
Activation energy $Q$		226.9 kJ mol <sup>-1</sup>	
Initial packing density 55%		Initial packing density 69%	
a	43.346	a	26.005
b	0.144853	b	0.334145
c	0.127167	c	3.100600
$\rho_o$	56.12%	$\rho_o$	69.49%
Log ( $\Theta_o$ )	-8.150293	Log ( $\Theta_o$ )	-10.497811
The master grain growth curve			
Activation energy $Q_G$		288013.3 kJ mol <sup>-1</sup>	
Initial packing density 55%		Initial packing density 69%	
$K_G$	$4.9539 \times 10^{-12}$	$K_G$	$3.4889 \times 10^{-12}$

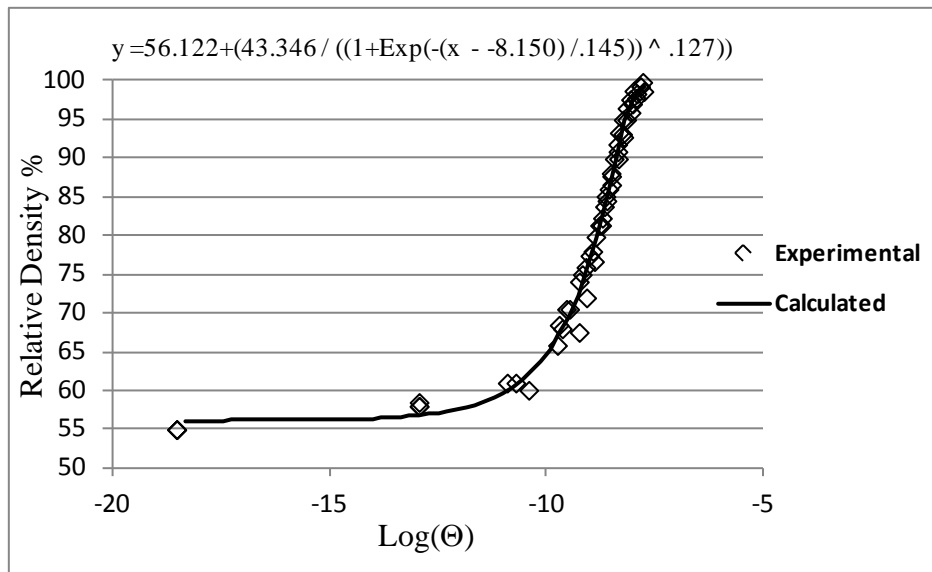


**Figure No (1) : The master sintering curve for  $\text{TiO}_2$  compacts of initial packing density of 55% of theoretical.**

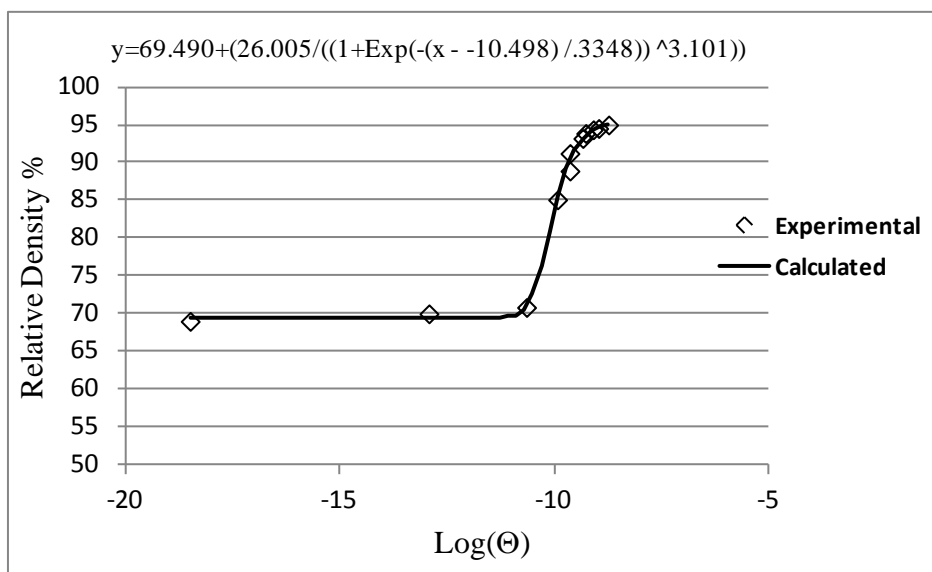


**Figure No. (2) : The master sintering curve for  $\text{TiO}_2$  compacts of initial packing density of 69 % of theoretical**

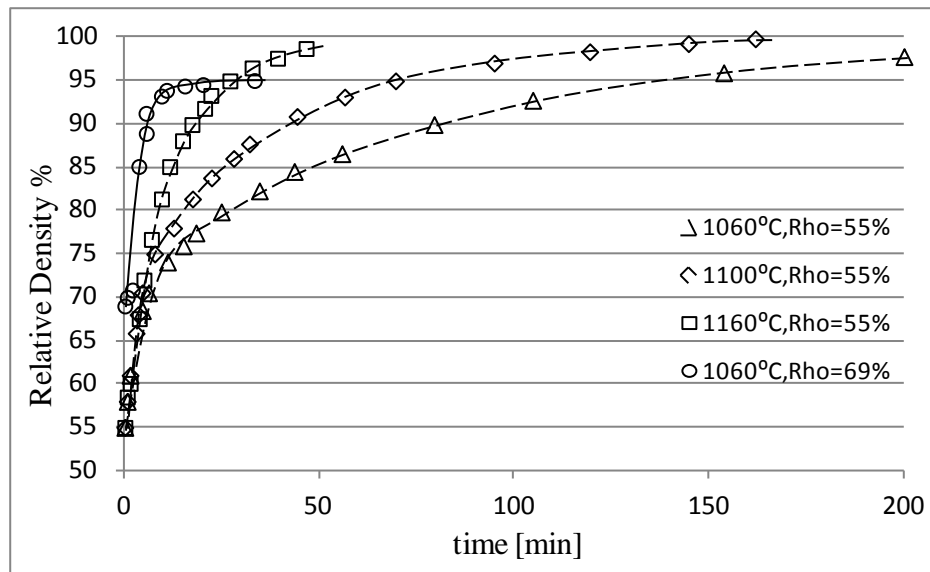


**Figure No (3) : The density-time trajectories for the sintered  $\text{TiO}_2$  compacts of initial packing density of 55% and 69% of theoretical. The data labels represent the input data for the model and the lines is the calculated. The dash lines are for 55% initial packing density and the solid line is for the 69% packing density**

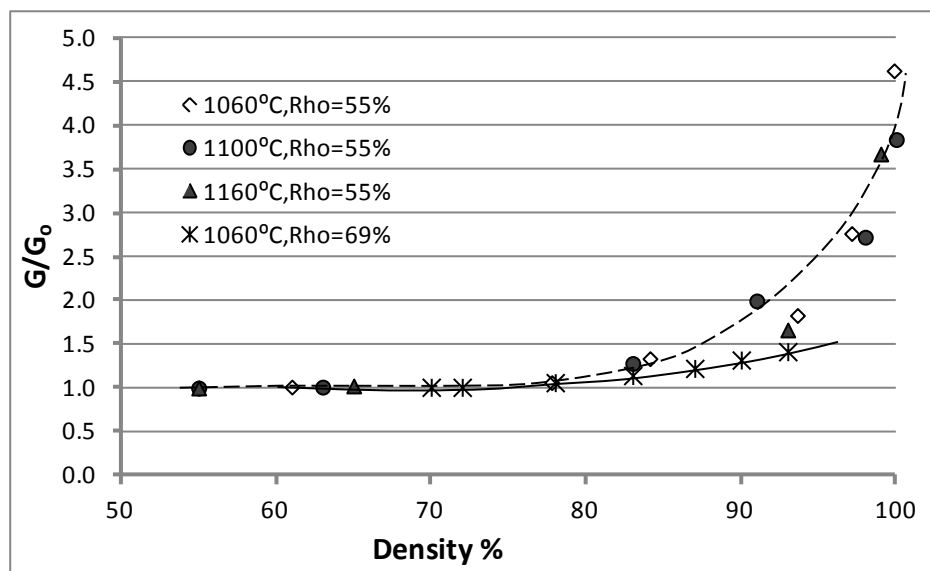


**Figure No (4) : The master grain growth curve for  $\text{TiO}_2$  compacts. The data labels represent the input data for the model and the lines is the calculated. The dash lines are for 55% initial packing density and the solid line is for the 69% packing density**

## منحنى التلييد الحاكم الى $TiO_2$

سعد بدري حسون فريد

قسم هندسة المواد / الجامعة التكنولوجية

سوسن عبد الحسين مهدي

حنان كاظم حسون

قسم الفيزياء/ كلية التربية للعلوم الصرفة /أبن الهيثم /جامعة بغداد

أستلم في : 9كانون الاول 2012 قبل في : 17 آذار 2013

### الخلاصة

قدم مفهوم منحنى التلييد الحاكم نموذج يوحد المرحلة الابتدائية والوسطية والنهائية للتلييد. لايعتمد منحنى التلييد الحاكم على منحنى الحرارة وزمن التلييد لانه يتعامل مع تكامل الحرارة مع الزمن. ويتم بناء منحنى التلييد الحاكم على عامل خاص بنوع المادة وهو طاقة التنشيط الخاصة بالتلييد ويعتمد هذا المنحنى كذلك على عوامل اخرى تؤثر في شكل المنحنى وتعتمد على الحالة الاولى للمضغوطات. استخدمت قيم منشورة لتلييد مضغوطات مسحوق اوكسيد التيتانيوم ذات كثافات رص اولية بمقدار 55% و69% من الكثافة النظرية لبناء منحنى التلييد الحاكم. بينت المضغوطة ذات كثافة الرص الاعلى معدل تكاثف أعلى، التي انعكست من خلال قيم مختلفة للعوامل التي تؤثر في شكل منحنى التلييد الحاكم مقارنة بتلك الخاصة بتلييد المضغوطات ذات كثافة الرص الابتدائية الأقل. وتم كذلك بناء منحنى النمو الحبيبي الحاكم لمضغوطات اوكسيد التيتانيوم الذي بين نمو حبيبي ابطاً للمضغوطة ذات كثافة الرص الأعلى.

الكلمات المفتاحية التلييد ، منحنى التلييد الحاكم، اوكسيد التيتانيوم